Res Chem Intermed
DOI 10.1007/s11164-016-2668-7

Cyclodextrin nanosponges: a potential catalyst and catalyst support for synthesis of xanthenes

Samahe Sadjadi[1] · **Majid M. Heravi**[2] · **Mansoureh Daraie**[2]

Received: 5 June 2016 / Accepted: 15 July 2016

Abstract The nanoporous framework of a cyclodextrin nanosponge was used as catalyst for accelerating the one-pot, three-component reaction of dimedone, aldehyde, and phenols for synthesis of xanthene derivatives. Moreover, the nanocavities of cyclodextrin nanosponges were exploited for immobilization of heteropolyacids through the wet impregnation method. This catalyst exhibited superior catalytic performance compared to the bare cyclodextrin nanosponge. Despite the good catalytic activity, the leaching of the catalytic species did not allow efficient recovery and reusability. To circumvent this problem, the cyclodextrin nanosponge was amine-functionalized prior to heteropolyacid immobilization. The results proved that the amine functionalities had an effective role in preserving the catalytic species and improving the reusability through decreasing the leaching time. This catalyst was used for synthesis of a variety of xanthenes in aqueous media. The catalytic amount of catalyst afforded the desired product in excellent yields and with a relatively short reaction time. The results suggested cyclodextrin nanosponge-based catalysts as potential candidates for promoting chemical reactions.

Keywords Heteropolyacids · Cyclodextrin nanosponge · Heterogeneous catalyst · Xanthenes

✉ Samahe Sadjadi
samahesadjadi@yahoo.com

✉ Majid M. Heravi
mmh1331@yahoo.com

1 Gas Conversion Department, Faculty of Petrochemicals, Iran Polymer and Petrochemical Institute, PO Box 14975-112, Tehran, Iran

2 Department of Chemistry, School of Science, Alzahra University, PO Box 1993891176, Vanak, Tehran, Iran

Introduction

Cyclodextrin (CD)-nanosponges, CDNS, are a class of hyper-crosslinked polymers with porosity arising from CD nano-sized cavities and interconnecting voids [1]. Unlike CDs, which are capable of hosting guests with compatible polarity and geometry, CDNS three-dimensional scaffolds can encapsulate a wide range of hydrophobic and hydrophilic molecules [2]. Recently, CDNS have been considered as potential nano-carriers for drug delivery purposes [3–5] due to their promising features such as insolubility in most organic solvents, tuneability of their porosity, stability at high temperature and wide pH range [1, 6]. Inclusion complexes of drugs with these nanoporous systems can improve the solubility and bioavailability of drugs and result in prolonged release. CDNS have also been considered as potential candidates for removal of hazardous chemicals from water [7]. Despite the interesting characteristics of CDNS, there are only a few reports on their applications for catalysis [8, 9], most of them related to enzyme immobilization [10, 11].

Xanthene derivatives are of an attractive class of heterocycles that can be found in various biologically active compounds [12]. These heterocycles possess numerous biological properties [13] including anti-inflammatory [14], antibacterial, and antiviral activities [15]. Moreover, xanthenes have interesting spectroscopic properties, which make them potential candidate for visualization of biomolecules [16], dye, laser technology [17], and photodynamic therapy [18]. To date, various methods and catalysts have been developed for synthesis of xanthenes [18–22].

Heteropolyacids, HPA, are of a non-toxic, non-corrosive, and environmentally friendly class of catalyst, which have been extensively used for their strong Bronsted acidity and redox potential [23]. The utility of HPA catalysts for promoting various chemical reactions such as oxidation [24, 25], hydrolysis [26], and reduction [27] has been proved.

In this paper, the catalytic activity of CDNS for synthesis of xanthene derivatives in aqueous media and with mild reaction time has been revealed (Scheme 1).

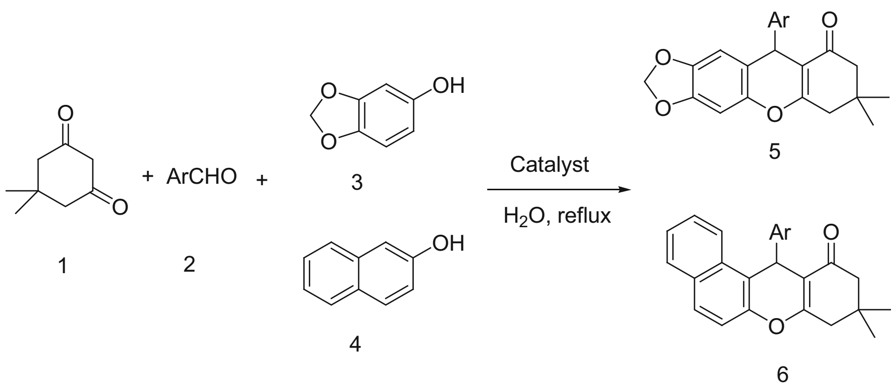

Scheme 1 Synthesis of xanthene derivatives

Furthermore, CDNS and functionalized CDNS, $CDNS/NH_2$, are used for embedding Keggin type HPA, $H_4[Mo_{12}PO_{40}]$, to develop novel catalysts, HPA-CDNS and HPA-$CDNS/NH_2$.

Experimental

Synthesis of CDNS

CDNS was prepared through modification of a previously reported procedure [28–30]. Briefly, 1 mmol of β-cyclodextrin was pre-heated at 100 °C for 2 h and then added slowly to the molten mixture of 2 mmol diphenyl carbonate (Scheme 2). The mixture was stirred vigorously at 120 °C for 12 h. The white product formed at the initial stage of the reaction was manually crushed and mixed with other reagents to make them react more effectively. The prolonged reaction time and elevated reaction temperature transformed the white solid into a colorless gel-like compound. After completion of reaction, the product was cooled to room temperature and milled. Un-reacted β-cyclodextrin and byproducts such as phenol were removed by washing the solid with distilled water and acetone, respectively. Further purification was carried out by soxhlet extraction with ethanol. The white powder was dried overnight in an oven at 60 °C.

Synthesis of $CDNS/NH_2$

A simple post-synthesis method was used for functionalization of CDNS. In a typical process, 1.0 g of synthesized CDNS was reacted with 50 mL of 0.02 M solution of 3-aminopropyl-triethoxysilane, APTES, in dried toluene under reflux for 24 h. The obtained precipitate, denoted as $CDNS/NH_2$, was filtered off and washed several times with dried toluene and subsequently dried at 70 °C for 8 h.

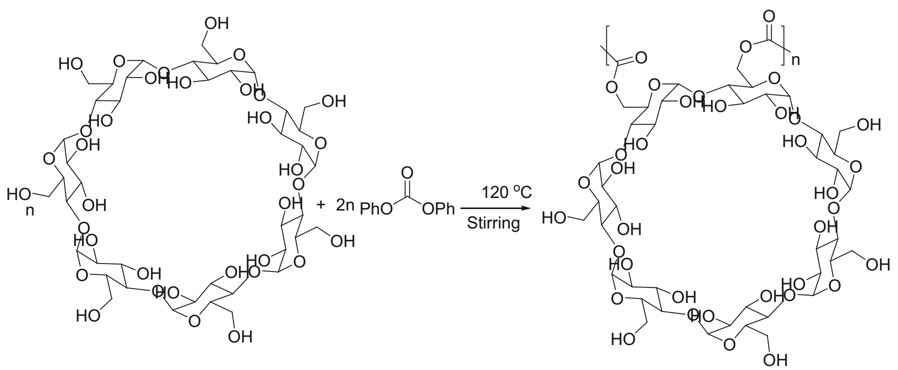

Scheme 2 Schematic illustration of synthesis of CDNS

Immobilization of HPA

The immobilization of HPA was obtained by using an incipient wetness impregnation method. $H_4[Mo_{12}PO_{40}]$ was dissolved in deionized water, and then added slowly to the suspension of CDNS or CDNS/NH_2 in deionized water. The sample was subjected to ultrasonic irradiation for half an hour and subsequently impregnated for 24 h at room temperature and dried in oven at 70 °C. The weight percentage of heteropolyacids loading was 20 % (w/w).

Synthesis of xanthene derivatives: General procedure

A solution of an appropriate aromatic aldehyde (1 mmol), dimedone (1 mmol), 3,4-methylene-dioxy-phenol or β-naphthol (1 mmol), and catalyst (0.02 g) in H_2O (5 mL) was refluxed for an appropriate time. After completion of the reaction, monitored by TLC, the catalyst was separated by simple filtration, and the mixture was cooled to room temperature. The percipitated solid was filtered off and washed with water and purified by recrystallization from absolute ethanol. All products were known and identified by comparison of their physical and spectroscopic data with those of authentic samples, which were found to be identical.

Characterization of CDNS

The synthesized catalysts were characterized by using SEM/EDX, BET, XRD, FTIR, and TGA techniques. SEM/EDX images of the catalysts were taken by a Tescan instrument, using Au-coated samples and an acceleration voltage of 20 kV. Room temperature powder X-ray diffraction patterns were collected using a Philips X-ray Diffractometer. Cu CuKα radiation was used from a sealed tube. Data were collected in the 2θ range 10°–88° with a step of 0.02 and an exposure per step of 2 s. BET surface areas were determined via nitrogen physisorption using a Brunauer Emmett Teller—BELSORP Mini II sorption analyzer (Micromeritics) at 77 K. The samples were activated at 100 °C for 4 h prior to measurements. Thermal analyses were performed using a Mettler analyzer. FTIR analyses were carried out by employing a PERKIN-ELMER-Spectrum 65 instrument.

Result and discussion

Characterization of catalysts

Characterization of CDNS

The formation of CDNS was confirmed by FTIR spectroscopy (Fig. 1). The appearance of a new peak at 1770 cm^{-1} which is the characteristic peak of the carbonate functional group, established the formation of a nanosponge scaffold. The SEM images of CDNS, Fig. 2, revealed the layered structure of nanosponges. The BET surface area of CDNS is reported in Table 1. As expected from the previous

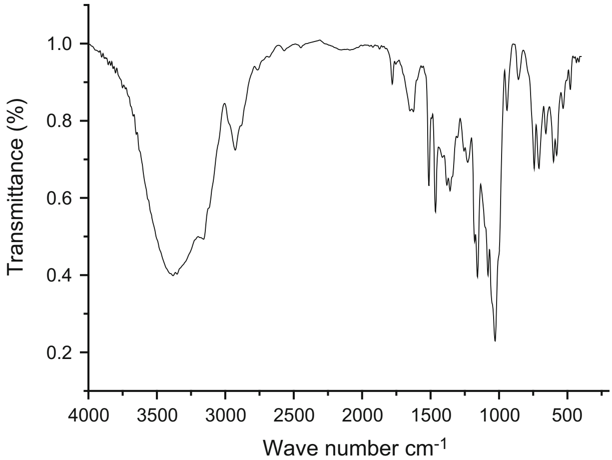

Fig. 1 FTIR spectrum of CDNS

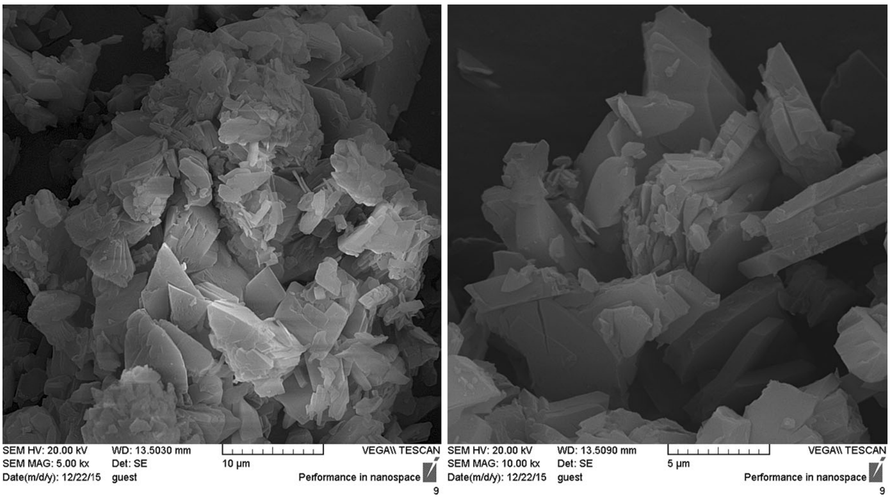

Fig. 2 SEM image of CDNS

reports [2], low surface area was obtained for synthesized CDNS. However, the measured value was much higher than those of reported ones (1–2 $m^2\ g^{-1}$) [2].

Characterization of CDNS/NH$_2$

As the FTIR spectra of CDNS and CDNS/NH_2 were almost similar, this analysis cannot clearly confirm the conjugation of APTES to CDNS. Therefore, SEM/EDX analysis was used to elucidate the formation of amine functionalized CDNS, CDNS/NH_2 (Figs. 3, 4). The presence of N and Si atoms in the EDX analysis demonstrated the formation of CDNS/NH_2.

Table 1 Textural parameters of CDNS and HPA-CDNS from N_2 adsorption isotherms

Sample	S_{BET} ($m^2\ g^{-1}$)	Average pore diameter (nm)	Total pore volume ($cm^3\ g^{-1}$)
CDNS	9.70	11.18	0.027
HPA-CDNS	8.62	12.59	0.027
HPA-CDNS/NH_2	3.42	14.26	0.012

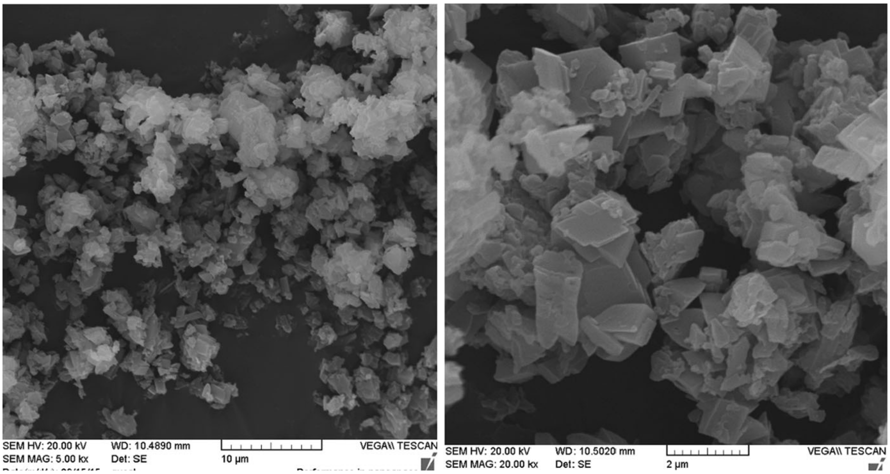

Fig. 3 SEM images of CDNS/NH_2

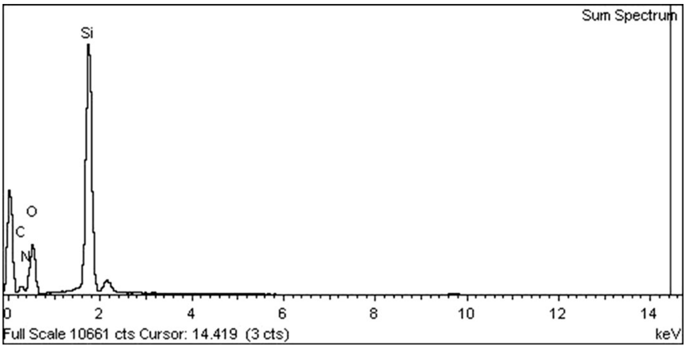

Fig. 4 EDX analysis of CDNS/NH_2

Characterization of HPA-CDNS

The SEM/EDX analyses (Figs. 5, 6) of HPA-impregnated CDNS, HPA-CDNS, demonstrated the presence of HPA onto CDNS. Furthermore, the SEM images of HPA-CDNS are clearly different from the bare CDNS. The XRD pattern of HPA-CDNS, illustrated in Fig. 7, indicated the relatively crystalline structure of the HPA-

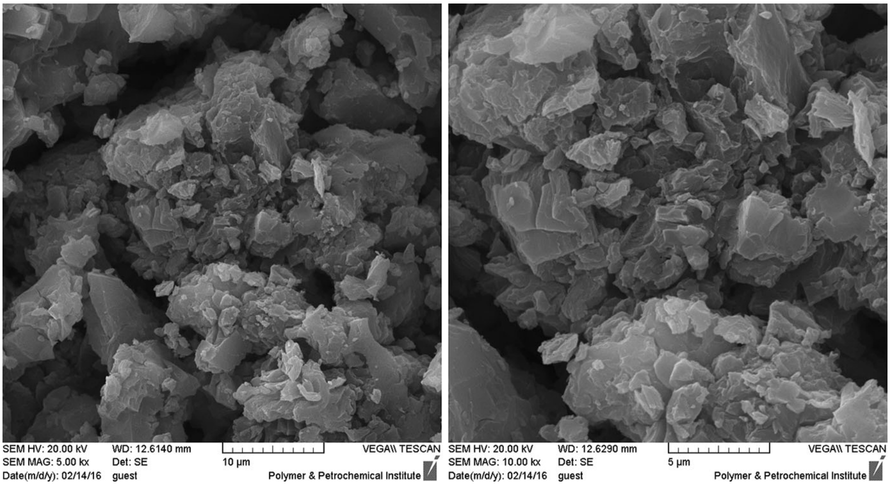

Fig. 5 SEM images of HPA-CDNS

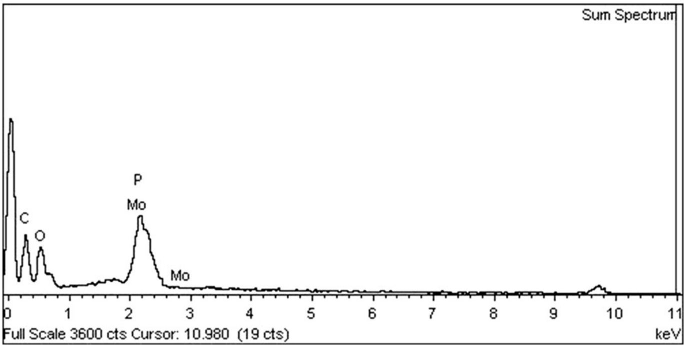

Fig. 6 EDX analysis of HPA-CDNS

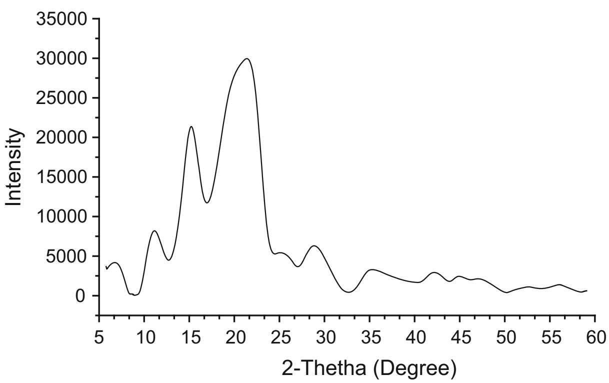

Fig. 7 XRD pattern of HPA-CDNS

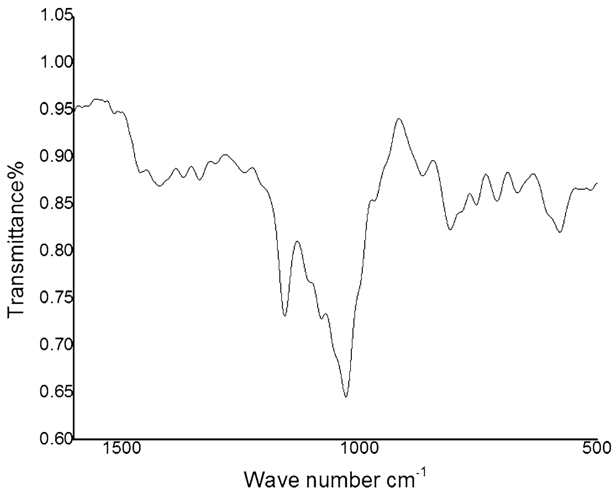

Fig. 8 FTIR spectrum of HPA-CDNS

CDNS. The FTIR spectrum of HPA-CDNS is shown in Fig. 8. The peaks at 1085, 875, 798, and 962 cm^{-1} can be assigned to symmetric stretching of P–O, Mo–Oc–Mo, Mo–Oe–Mo, and Mo–Ot, respectively. The BET surface area of HPA-CDNS, reported in Table 1, demonstrates that the surface area and total pore volume of HPA-CDNS are lower than those of bare CDNS, indicating that HPA resided not only on the surface of the CD but also within its pores. The higher average pore diameter observed for HPA-CDNS could presumably emerge from confinement of HPA within the cavities of CDNS. The gravimetric thermal analysis, TGA, of the synthesized CDNS is illustrated in Fig. 9. This analysis clearly demonstrated that HPA-CDNS was thermally stable and no degradation was observed until 290 °C. Comparison of gravimetric thermal analysis of HPA-CDNS with the reported TGA of bare CDNS, in which degradation was not reported until 340 °C, indicated that incorporation of HPA in CDNS can slightly decrease thermal stability.

Characterization of HPA-CDNS/NH_2

The SEM images of HPA-CDNS/NH_2 are shown in Fig. 10. These images are clearly distinguished from SEM images of HPA-CDNS, indicating the effect of functionalization of CDNS on the morphology and dispersion of HPA. The XRD pattern and TGA analysis are depicted in Figs. 11 and 12, respectively. The XRD pattern established the relative crystalline structure of HPA-CDNS/NH_2. This pattern is almost similar to that of HPA-CDNS. As shown in Fig. 12, the degradation was occurring at 300 °C. The measurement of BET surface area of HPA-CDNS/NH_2 (Table 1) indicated the decreased values of surface area and total pore volume of HPA-CDNS/NH_2 compared to the bare CDNS and HPA-CDNS. This observation can confirm the fact that functionalized CDNS can embed HPA more effectively through additional attractive interactions. The decreased value of

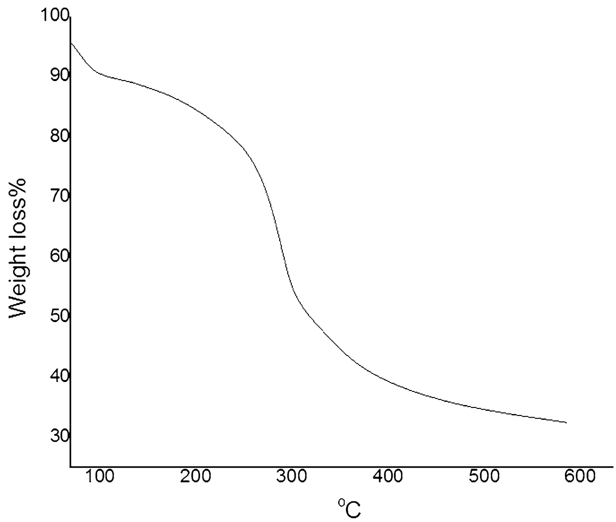

Fig. 9 TGA analysis of HPA-CDNS

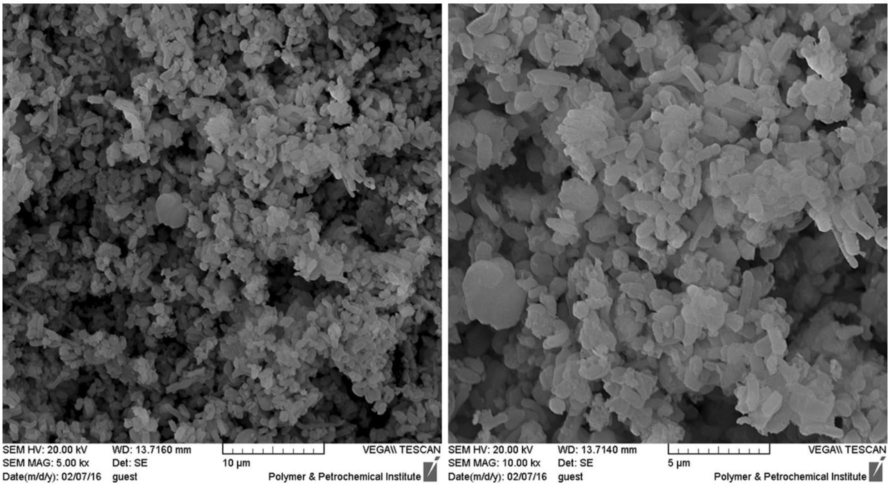

Fig. 10 SEM images of HPA-CDNS/NH_2

the average pore diameter can be attributed to functionalization of interior hydroxy groups and encapsulation of HPA within the pores of a porous structure.

According to previous reports [2], carbamate CDNS possesses a high loading capacity for a broad range of organic species despite their very low surface area (1–2 m^2 g^{-1}). This characteristic was attributed to the fact that loading of molecules does not proceed through a conventional surface adsorption but transportation into the bulk of CD-nanosponges. The inclusion is a downhill process, which occurs spontaneously with ΔG° 10–13 kcal mol^{-1} (at 298 K) [2].

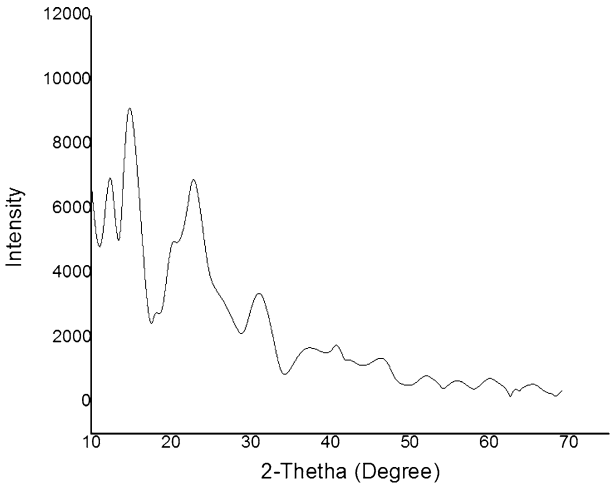

Fig. 11 XRD pattern of HPA-CDNS/NH_2

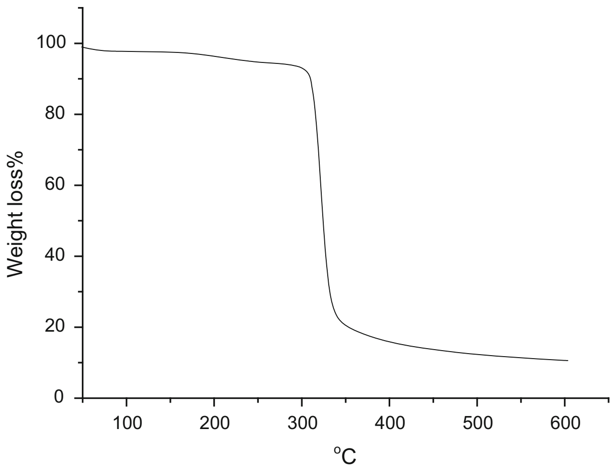

Fig. 12 TGA analysis of HPA-CDNS/NH_2

Based on this knowledge, we initially examined whether CDNS can promote chemical reaction of organic substrate through formation of an inclusion complex with substrates and concentrating them within the CDNS cavities. To this purpose, synthesis of 7,8-dihydro-10-phenyl-7,7-dimethyl-6*H*-[1,3]dioxolo[4,5-*b*]xanthen-9(10*H*)-one was selected as a model reaction and performed in aqueous media under reflux conditions in the presence of CDNS as a catalyst. The reaction conditon, i.e., solvent and catalyst amount were optimized. Gratifingly, CDNS promoted the model reaction under optimized reaction conditions and afforded the desired product in 75 % yield after 3.5 h. The observed catalytic activity that was higher than some conventional catalysts such as DABCO and sulfuric acid

Table 2 The catalytic activities of various catalysts for the synthesis of 7,8-dihydro-10-phenyl-7,7-dimethyl-6*H*-[1,3]dioxolo[4,5-b]xanthen-9(10*H*)-one under reflux conditions

Entry	Catalyst	Solvent	Temp.	Time (h)	Yield (%)[a]
1	$H_{14}NaP_5W_{30}O_{110}$	Water	Reflux	2	80
2	Sulfamic acid	Water	Reflux	3	75
3	DABCO	Water	Reflux	4	60
4	CDNS	Water	Reflux	3.5	75
7	HPA-CDNS	Water	Reflux	1.5	90

[a] The proposed mechanism of formation of xanthenes

(Table 2), not only can be attributed to the formation of an inclusion complex of substrates and CDNS and concentrating substrates, but also to the contribution of CDNS to promoting the reaction through formation of hydrogen bonds with substrate. This can be better explained by considering the reaction mechanism (Scheme 3). Initially dimedone and aldehyde tolerated the Knoevenagle condensation to afford an intermediate. Subsequent reaction of the latter with phenol followed by dehydration will furnish the desired product. The numerous hydroxy groups present in the CDNS scaffold can promote the hydrogen bonds with aldehyde and accelerate the Knoevenagle condensation and coupling of phenol in the next step. Additionally, the ability of forming hydrogen bonds can facilitate the generation of an inclusion complex.

To study the generality of this procedure, various derivatives of 5 were synthesized in the presence of catalytic amounts of CDNS (Table 3). The results demonstrated high catalytic activity of CDNS.

To expand the catalytic utility of CDNS, its utility as a catalytically active support for catalyst immobilization was also examined. In our previous work, we disclosed that HPA could be considered as an efficient catalyst for the synthesis of xanthan derivatives [20]. Armed with this experience, we embedded HPA onto CDNS, which can serve as a porous support to afford a novel catalyst, HPA-CDNS. The catalytic activity of this catalyst was evaluated for the model reaction (Table 4). The result demonstrated the superior catalytic activity of HPA-CDNS compared to

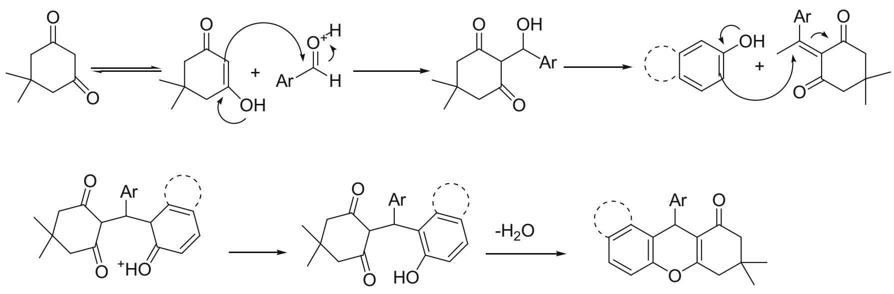

Scheme 3 Synthesis of xanthene derivatives

Table 3 Synthesis of **5a–h** using a catalytic amount of CDNS

Entry	Ar	Product	Time (h)	Yield (%)[a]	M.p (°C)	M.p. rep (°C) [20]
1	C_6H_5	**5a**	1.5	90	189–192	190–192
2	4-NO_2–C_6H_4	**5b**	2	92	200–203	201–202
3	4-MeO–C_6H_4	**5c**	2.2	90	165–197	197–198
4	3-NO_2–C_6H_4	**5d**	2.5	88	153–156	156–158
5	3-MeO–C_6H_4	**5f**	2.7	87	140–142	141–142
6	2-Me–C_6H_4	**5g**	3	90	177–180	176–178
7	2,4-Cl_2–C_6H_3	**5h**	2	88	213–214	214–215

[a] The proposed mechanism of formation of xanthenes

Table 4 Optimization of the reaction solvent for the synthesis of 7,8-dihydro-10-phenyl-7,7-dimethyl-6*H*-[1,3] dioxolo[4,5-b]xanthen-9(10*H*)-one by using HPA-CDNS under reflux conditions

Entry	Catalyst	Solvent	Temp.	Time (h)	Yield (%)[a]
5	HPA-CDNS	EtOH	Reflux	2.5	85
	HPA-CDNS	CH_3CN	Reflux	3	85
7	HPA-CDNS	Water	Reflux	1.5	90

[a] The proposed mechanism of formation of xanthenes

the bare CDNS. This result can be rationalized based on the synergetic effects of catalytic active sites, HPA (Bronsted acidity), and CDNS.

The reaction condition was optimized by using the model reaction (Table 4). Initially the model reaction was carried out in various solvents including water, ethanol, and acetonitrile. Gratifingly, the highest catalytic activity and shortest reaction time were obtained in the presence of water as a green and economical solvent.

The effect of catalyst amount was also studied by using 0.01–0.04 g of catalyst per 1 mmol of reagents. The optimum amount of catalyst was obtained as 0.02 g.

The scope of the reaction was studied by using a variety of substrates with different electronic properties under optimized reaction conditions (Tables 5, 6). The results indicated that the substrates with both electron-donating and electron-withdrawing groups could lead to high yields in a relatively short reaction time.

It is worth noting that CDNS can be recovered simply and reused. In the case of HPA-CDNS, however, as the interaction between HPA and CDNS are weak electrostatic and van der Waals interactions, the catalyst leaching was inevitable, and the loss of catalytic activity was observed upon recycling and reusing. To circumvent this problem and improve the reusability of the catalyst, CDNS was functionalized by APTES prior to impregnation to afford new a catalyst, HPA-CDNS/NH_2. It was postulated that stronger interactions of HPA in the case of functionalized CDNS could decrease the leaching and result in a more stable heterogeneous catalyst. Syntheses of various derivatives of compounds **5** and **6** were carried out in the presence of catalytic amounts of HPA-CDNS/NH_2. The results

Table 5 Synthesis of **5a–h** using a catalytic amount of HPA-CDNS

Entry	Ar	Product	Time (h)	Yield (%)[a]	M.p (°C)	M.p. rep (°C) [20]
1	C_6H_5	**5a**	1.5	90	189–192	190–192
2	4-NO_2–C_6H_4	**5b**	2	92	200–203	201–202
3	4-MeO–C_6H_4	**5c**	2.2	90	165–197	197–198
4	3-NO_2–C_6H_4	**5d**	2.5	88	153–156	156–158
5	3-MeO–C_6H_4	**5f**	2.7	87	140–142	141–142
6	2-Me–C_6H_4	**5g**	3	90	177–180	176–178
7	2,4-Cl_2–C_6H_3	**5h**	2	88	213–214	214–215

[a] The proposed mechanism of formation of xanthenes

Table 6 Synthesis of **6a–i** using a catalytic amount of HPA-CDNS

Entry	Ar	Product	Time (h)	Yield (%)[a]	M.p (°C)	M.p. rep (°C) [20]
1	C_6H_5	**6a**	2.5	90	153–155	154–155
2	4-Cl–C_6H_4	**6b**	2	95	184–186	185–187
3	4-Br–C_6H_4	**6c**	2	90	185–187	186–188
4	4-NO_2–C_6H_4	**6d**	2.5	92	182–185	183–184
5	4-MeO–C_6H_4	**6e**	2.7	90	189–201	200–202
6	3-NO_2–C_6H_4	**6f**	3	88	170–172	172–174
7	3-MeO–C_6H_4	**6g**	3	87	202–203	204–205
8	2-Me–C_6H_4	**6h**	3.2	90	159–160	159–162
7	2,4-Cl_2–C_6H_3	**6i**	2.7	88	213–214	214–215

[a] The proposed mechanism of formation of xanthenes

Table 7 Synthesis of **5a–h** using a catalytic amount of HPA-CDNS/NH_2

Entry	Ar	Product	Time (min)	Yield (%)[a]	M.p (°C)	M.p. rep (°C) [20]
1	C_6H_5	**5a**	40	94	189–192	190–192
2	4-NO_2–C_6H_4	**5b**	45	92	200–203	201–202
3	4-MeO–C_6H_4	**5c**	50	93	165–197	197–198
4	3-NO_2–C_6H_4	**5d**	45	89	153–156	156–158
5	3-MeO–C_6H_4	**5f**	50	90	140–142	141–142
6	2-Me–C_6H_4	**5g**	60	92	177–180	176–178
7	2,4-Cl_2–C_6H_3	**5h**	45	93	213–214	214–215

[a] The proposed mechanism of formation of xanthenes

(Table 7 and 8) proved the superior catalytic activity of HPA-CDNS/NH_2 compared to HPA-CDNS. All products were obtained in excellent yields in a shorter reaction time. The observed superior catalytic activity can be assigned to better dispersion and immobilization of HPA onto CDNS/NH_2 due to conjugation of APTES, which

Table 8 Synthesis of **6a–i** using a catalytic amount of HPA-CDNS/NH_2

Entry	Ar	Product	Time (min)	Yield (%)[a]	M.p (°C)	M.p. rep (°C) [20]
1	C_6H_5	**6a**	60	91	153–155	154–155
2	4-Cl–C_6H_4	**6b**	55	94	184–186	185–187
3	4-Br–C_6H_4	**6c**	55	94	185–187	186–188
4	4-NO_2–C_6H_4	**6d**	45	93	182–185	183–184
5	4-MeO–C_6H_4	**6e**	50	94	189–201	200–202
6	3-NO_2–C_6H_4	**6f**	60	90	170–172	172–174
7	3-MeO–C_6H_4	**6g**	70	91	202–203	204–205
8	2-Me–C_6H_4	**6h**	75	90	159–160	159–162
7	2,4-Cl_2–C_6H_3	**6i**	45	92	213–214	214–215

[a] The proposed mechanism of formation of xanthenes

can act both as anchor and spacer. Checking the reusability of this catalyst proved its superior recovery and reusability compared to HPA-CDNS. However, leaching of catalytic species, HPA, was not completely suppressed and loss of activity was observed upon reusing the catalyst after several reaction runs.

It is worth noting that in this study synthesis of xanthan derivatives was selected as an organic reaction to investigate the utility of CDNS-based systems for catalysis. Although in some previous reports the synthesis of xanthans was reported in slightly higher yields and shorter reaction times [31], the promising results from the present study proved that the nanocavities of porous CDNS can be considered as efficient catalysts with possible applications for catalyzing not only xanthans but also various chemicals. Moreover, it has been shown that the properties of CDNS can be tuned by simple post treatment to allow effective embedding of catalytically active species and developing new hybrid catalysts.

Conclusion

In summary, the utility of CDNS both as a catalyst and a catalyst support for immobilization of HPA for synthesis of xanthenes has been proved. The observed catalytic activity was attributed to the formation of an inclusion complex between CDNS and reagents, which is a downhill process, and formation of hydrogen bonds between hydroxyl groups of CDNS and reagents. The synergetic effect of the embedded HPA and CDNS can rationalize the superior activity of HPA-CDNS. To improve the catalyst reusability and suppress HPA leaching, CDNS was functionalized with APTES to afford HPA-CDNS/NH_2. This novel catalyst exhibited superior catalytic performance in terms of reactivity and reusability. The green and mild reaction condition, excellent yields, and broad substrate scope are the merits of this novel procedure. The catalytic activity of CDNS-based catalysts for xanthan synthesis proved the potential use of the nanocavities of CDNS for hosting catalytic species and developing novel hybrid catalysts. More research for developing a true heterogeneous catalyst based on functionalized CDNS is under way.

Acknowledgments The authors appreciate partial financial support from Iran Polymer and Petrochemical Institute and Alzahra University. MMH is also thankful to INSF for financial support given under cover of given individual grant.

References

1. G. Tejashri, B. Amrita, J. Darshana, Acta Pharm. **63**, 335 (2013)
2. F. Trotta, in *Cyclodextrins in Pharmaceutics, Cosmetics, and Biomedicine: Current and Future Industrial Applications*, ed. by E. Bilensoy (Wiley, Hoboken, 2011), p. 323
3. S. Anandam, S. Selvamuthukumar, J. Mater. Sci. **49**, 8140 (2014)
4. P. Shende, K. Deshmukh, F. Trotta, F. Caldera, Int. J. Pharm. **456**, 95 (2013)
5. S. Torne, S. Darandale, P. Vavia, F. Trotta, R. Cavalli, Pharm. Dev. Technol. **18**, 619 (2013)
6. M. Shringirishi, S.K. Prajapati, A. Mahor, S. Alok, P. Yadav, A. Verma, Asian. Pac. J. Trop. Dis. **4**, S519 (2014)
7. M. Arkas, R. Allabashi, D. Tsiourvas, E.-M. Mattausch, R. Perfle, Environ. Sci. Technol. **40**, 2771 (2006)
8. G. Cravotto, E.C. Calcio Gaudino, S. Tagliapietra, D. Carnaroglio, A. Procopio, Green Process. Synth. **1**, 269 (2012)
9. P. Cintas, G. Cravotto, E.C. Gaudino, L. Orio, L. Boffa, Catal. Sci. Technol. **2**, 85 (2012)
10. G. Di Nardo, C. Roggero, S. Campolongo, F. Valetti, F. Trotta, G. Gilardi, Dalton Trans. **7**, 6507 (2009)
11. B. Boscolo, F. Trotta, E. Ghibaudi, J. Mol. Catal. B Enzym. **62**, 155 (2010)
12. A. Gharib, L. Vojdani Fard, N.N. Pesyan, M. Roshani, Chem. J. **1**, 58 (2015)
13. J.M. Khurana, D. Magoo, K. Aggarwal, N. Aggarwal, R. Kumar, C. Srivastava, Eur. J. Med. Chem. **58**, 470 (2012)
14. J.M. Jamison, K. Krabill, A. Hatwalkar, Cell Biol. Int. Rep. **14**, 1075 (1990)
15. R.M. Ion, D. Frackowiak, K. Wiktorowicz, Acta Biochim. Pol. **45**, 833 (1998)
16. O. Evangelinou, A.G. Hatzidimitriou, E. Velalib, A.A. Pantazaki, N. Voulgarakis, P. Aslanidis, Polyhedron **72**, 122 (2014)
17. O. Sirkecioglu, N. Talinli, A. Akar, J. Chem. Res. 502 (1995)
18. P. Bansal, G.R. Chaudhary, N. Kaur, S.K. Mehta, RSC Adv. **5**, 8205 (2015)
19. G.R. Chaudhary, P. Bansal, N. Kaur, S.K. Mehta, RSC Adv. **4**, 49462 (2014)
20. M.M. Heravi, H. Alinejhad, K. Bakhtiari, M. Saeedi, H.A. Oskooie, F.F. Bamoharram, Bull. Chem. Soc. Ethiop. **25**, 399 (2011)
21. K. Rad-Moghadam, S.K. Azimi, J. Mol. Catal. A: Chem. **363–364**, 465 (2012)
22. N.G. Khaligh, Ultrason. Sonochem. **19**, 736 (2012)
23. M.M. Heravi, S. Sadjadi, J. Iran. Chem. Soc. **6**, 1 (2009)
24. E. Rafiee, F. Mirnezami, J. Mol. Liq. **199**, 156 (2014)
25. K. Pamin, M. Pronczuk, S. Basąg, W. Kubiak, Z. Sojka, J. Połtowicz, Inorg. Chem. Commun. **59**, 13 (2015)
26. S. Tsubaki, K. Oono, T. Ueda, A. Onda, K. Yanagisawa, T. Mitani, J.-I. Azuma, Bioresour. Technol. **144**, 67 (2013)
27. A. Srivani, P.S. Sai Prasad, N. Lingaiah, Catal. Lett. **142**, 389 (2012)
28. S. Swaminathan, L. Pastero, L. Serpe, F. Trotta, P. Vavia, D. Aquilano, M. Trotta, G.P. Zara, R. Cavalli, Eur. J. Pharm. Biopharm. **74**, 193 (2010)
29. R. Cavalli, F. Trotta, W. Tumiatti, J. Incl. Phenom. **56**, 209 (2006)
30. F. Trotta, R. Cavalli, K. Martina, M. Biasizzo, J. Vitillo, S. Bordiga, P. Vavia, K. Ansari, J. Incl. Phenom. Macrocycl. Chem. **71**, 189 (2011)
31. G. Mohammadi Ziarani, A.-R. Badiei, M. Azizi, Sci. Iran. **18**, 453 (2011)